The Cytoplasmic Region of Mouse FcγRIIb1, but Not FcγRIIb2, Binds Phospholipid Membranes†

Lixin Chen,‡ Gary J. Pielak, and Nancy L. Thompson*

Department of Chemistry, Campus Box 3290, University of North Carolina, Chapel Hill, North Carolina 27599-3290

Received March 24, 1998; Revised Manuscript Received December 2, 1998

ABSTRACT: The cytoplasmic regions of the mouse low-affinity FcγRII isoforms, FcγRIIb1 and FcγRIIb2, play key roles in signal transduction by mediating different cellular functions. The FcγRIIb1 (94 residues) and FcγRIIb2 (47 residues) cytoplasmic regions are generated by differential mRNA splicing in which a single aspartic acid residue in FcγRIIb2 is replaced by a 48-residue insert in FcγRIIb1. In previous work, quantities of the mFcγRIIb1 and mFcγRIIb2 cytoplasmic regions were generated, and their secondary structures were examined in different solutions with circular dichroism [Chen, L., Thompson, N. L., and Pielak, G. J. (1997) *Protein Sci. 6,* 1038−1046]. In the work described here, steady-state light scattering was used to investigate possible interactions of the two isolated cytoplasmic regions with phospholipid vesicles. Three phospholipid compositions were examined: phosphatidylserine/phosphatidylcholine (PS/PC) (25/75, mol/mol); phosphatidylinositol bisphosphate/phosphatidylcholine (PIP_2/PC) (25/75, mol/mol); and pure phosphatidylcholine (PC). Binding was examined in the presence and absence of Ca^{2+}. The mFcγRIIb1 cytoplasmic peptide binds PS/PC vesicles weakly in the absence of Ca^{2+} and more strongly in the presence of Ca^{2+}. For PIP_2/PC vesicles, the behavior is reversed; binding is weak in the presence of Ca^{2+} and stronger in its absence. The mFcγRIIb1 peptide also weakly binds pure PC vesicles, in a Ca^{2+}-independent manner. The mFcγRIIb2 cytoplasmic peptide does not bind, in the presence or absence of Ca^{2+}, to PS/PC, PIP_2/PC, or PC vesicles. The implications of these results for the mechanisms of signal transduction mediated by the two mFcγRII cytoplasmic regions are discussed.

Receptors for the Fc region of immunoglobulin G (Fcγ receptors) are primary cell-surface mediators of immune function *(1−7).* In mice and humans, at least three types of Fcγ receptors, FcγRI, FcγRII, and FcγRIII, have been identified. These three receptors differ in their affinities for IgG, cellular expression, and biological functions. This work focuses on mouse FcγRII (mFcγRII). There are two isoforms of mFcγRII, mFcγRIIb1 and mFcγRIIb2, which are products of the same gene and are generated by cell-type-specific mRNA splicing. Both isoforms have extracellular regions of two ≈90-residue Ig-like domains that bind the Fc region of IgG, a single 26-residue transmembrane domain, and a cytoplasmic tail of either 94 (mFcγRIIb1) or 47 (mFcγRIIb2) residues that participates in signal transduction. The primary structures of the two isoforms are identical except for an in-frame 48-residue insert in the cytoplasmic region of mFcγRIIb1, which replaces a single amino acid in mFcγRIIb2 (Figure 1).

mFcγRIIb2, which is expressed primarily on macrophages, mediates endocytosis of immune complexes *(8−12).* A 13 amino acid motif in the cytoplasmic region, called the immune receptor tyrosine-based inhibition motif (ITIM),[1] is responsible for coated pit localization and endocytosis.

```
          1          11         21         31         41
b1-94 KKKQVPALPGNPDHREMGETLPEEVGEYRQPSGGSVPVSPGPPS

          1
b2-47 KKKQVP----------------------------------------

          51         61         71         81         91
GLEPTSSSPYNPPDLEEAAKTEAENTITYSLLKHPEALDEETEHDYQNHI

                   11         21         31         41
---------DNPPDLEEAAKTEAENTITYSLLKHPEALDEETEHDYQNHI
```

FIGURE 1: Primary structures of mFcγRIIb1 and mFcγRIIb2 cytoplasmic regions. The amino acid sequences of the mFcγRIIb1 and mFcγRIIb2 cytoplasmic regions are identical except that a single aspartic acid residue (underline) in mFcγRIIb2 is replaced by a 48-residue insert in mFcγRIIb1. The 13 amino acid ITIM region is also underlined.

mFcγRIIb1 cannot trigger endocytosis even though it possesses this ITIM sequence. The 48 amino acid insert that distinguishes the mFcγRIIb1 isoform from the mFcγRIIb2 isoform appears to provide a negative signal that prevents coated pit localization and endocytosis. This negative signaling involves a putative interaction with the actin filaments in the cytoskeleton.

mFcγRIIb1, which is preferentially expressed in B lymphocytes, lacks immune complex internalization properties,

† This work was supported by National Institutes of Health Grants GM-37145 (N.L.T.) and GM-42501 (G.J.P.).

* To whom correspondence should be addressed: (919) 962-0328 (telephone), (919) 962-2388 (fax), nlt@unc.edu (e-mail).

‡ Present address: New England BioLabs, Inc., 32 Tozer Rd., Beverly, MA 01915.

[1] Abbreviations: b1−94, 94 amino acid cytoplasmic region of mFcγRIIb1; b2−47, 47 amino acid cytoplasmic region of mFcγRIIb2; ITIM, immune receptor tyrosine-based inhibition motif; PC, 1-palmitoyl-2-oleoyl-*sn*-glycero-3-phosphocholine; PIP_2, bovine brain phosphatidylinositol 4,5-bisphosphate; PS, bovine brain phosphatidylserine; Tris buffer, 50 mM Tris, 100 mM NaCl, pH 7.4 at 25 °C.

10.1021/bi980683j CCC: $18.00
Published on Web 01/23/1999

yet it inhibits B cell activation and subsequent antibody production when cross-linked to membrane Ig *(12−25)*. The down-regulation of B cell activation is correlated with tyrosine phosphorylation of mFcγRIIb1, inhibition of soluble IgG-stimulated Ca^{2+} influx, and decreased interleukin-2 secretion. Studies with deletion mutants locate the region that inhibits B cell activation to the 13 amino acid ITIM region that mediates immune complex endocytosis by mFcγRIIb2. The tyrosine in this motif (Figure 1) is phosphorylated upon cross-linking of mFcγRIIb1 with surface Ig, and mutation of this residue to phenylalanine abolishes the B cell inhibition. The mFcγRIIb1 ITIM prevents not only antigen-induced B cell activation but also T cell activation and FcϵRI-mediated mast cell activation.

Because the only structural difference between the two isoforms of mFcγRII occurs in the cytoplasmic region, it is reasonable to believe that this sequence difference plays an important mechanistic role. To investigate the relationship between the structure and function of the mFcγRIIb1 and mFcγRIIb2 cytoplasmic regions, we previously generated peptides corresponding to the cytoplasmic regions of mFcγRIIb1 and mFcγRIIb2 *(26)*. The mFcγRIIb1 cytoplasmic region was produced by overexpression in *E. coli* as a fusion peptide with maltose binding protein, purification of the fusion protein by affinity chromatography, enzymatic cleavage with thrombin to release the mFcγRIIb1 cytoplasmic peptide, and HPLC purification. The mFcγRIIb2 cytoplasmic region was chemically synthesized and purified by HPLC. The secondary structures of these two peptides in different solutions were examined with circular dichroism *(26)*. Here, steady-state light scattering has been used to investigate possible interactions of the two isolated cytoplasmic regions with phospholipid membranes. The results have implications for the mechanisms of signal transduction mediated by the two mFcγRII cytoplasmic regions.

MATERIALS AND METHODS

Peptides. The cytoplasmic regions of mFcγRIIb1 and mFcγRIIb2 (Figure 1) were generated as previously described *(26)*. A gene was constructed that contains (from the N terminal to the C terminal) the coding regions for maltose binding protein, a thrombin cleavage site, the mFcγRIIb1 cytoplasmic region, a methionine residue, and a six-residue histidine tag. The gene was expressed in *E. coli*, and the expressed protein was purified from cell lysates by affinity chromatography with nickel-chelation chromatography. Subsequent thrombin cleavage and HPLC purification yielded the mFcγRIIb1 cytoplasmic region containing the methionine and histidine tag. The cytoplasmic region of mFcγRIIb2 was chemically synthesized and purified by HPLC (TANA Laboratories, Houston, TX). The peptides are not modified at the N- or C-termini. Peptide concentrations were determined with a bicinchoninic acid assay (Pierce Chemical Co., Rockford, IL). The peptide molecular masses, calculated from the known amino acid sequences, are 10.2 kDa for b1−94 and 5.4 kDa for b2−47. At pH 7.4, the net charge of b1−94 is −11, and the net charge of b2−47 is −7. The protease inhibitor eglin c, containing a C-terminal, six-residue histidine tag, was generated as described elsewhere *(27)*.

Phospholipid Vesicles. 1-Palmitoyl-2-oleoyl-*sn*-glycero-3-phosphocholine (PC) (Avanti Polar Lipids, Birmingham, AL), bovine brain phosphatidylserine (PS) (Avanti), and bovine brain phosphatidylinositol 4,5-bisphosphate (PIP_2) (Calbiochem Corp., Cambridge, MA) were obtained commercially. Aliquots of phospholipids in chloroform were combined, dried with a vacuum concentrator to a thin film, and resuspended to 0.5 mM with Tris buffer (50 mM Tris, 100 mM NaCl, pH 7.4 at 25 °C). The lipid mixtures were sonicated (Model 300 Sonic Dismembrenator, Artek Systems, Farmingdale, NY) to clarity with ≈2 min pulses for a total of ≈30 min and then fractionated by centrifuging for 20 min at 130000*g* in an air ultracentrifuge (Beckman Instruments, Palo Alto, CA). The top half of the centrifuged vesicle suspension was used within 24 h. Vesicle compositions were either pure PC, PS/PC (25/75, mol/mol), or PIP_2/PC (25/75, mol/mol). Phosphate concentrations were determined by using a molybdenum-based assay *(28)*. The phospholipid molecular masses were 810.03 (PS), 1098.2 (PIP_2), and 760.1 (PC) g/mol.

Light Scattering Measurements. Peptide binding to phospholipid vesicles was examined by using steady-state light scattering *(29−32)*. Samples consisted of 1.5 mL of vesicles (0−200 μM phospholipid), peptides (0−20 μM), $CaCl_2$ (0−30 mM), and/or disodium ethylenedinitrilotetraacetic acid (EDTA) (0−100 mM) in Tris buffer. All solutions except phospholipid vesicle suspensions were passed through 0.2-μm filters immediately before use. The measurements were carried out on a spectrofluorimeter (Model 8000C, SLM Amino Instruments, Urbana, IL) in 90° format with both excitation and emission wavelengths of 320 nm. The samples were magnetically stirred, at room temperature, during data collection.

RESULTS

The intensities of light scattered by PS/PC, PIP_2/PC, and PC vesicles are linear with the phospholipid concentration up to at least 200 μM (Figure 2a). Similar results are observed for b1−94 and b2−47 peptides up to 10 μM (Figure 2b). This linearity is consistent with theoretical predictions for light scattering by low concentrations of particles that are much smaller than the light wavelength *(29−32)*. In this case, the scattered intensities are given by

$$I_{v,p} = \sigma_{v,p} C_{v,p} \quad (1)$$

where $c_{v,p}$ are concentrations, $\sigma_{v,p}$ are slopes, and the subscripts "v" and "p" denote vesicles and peptides, respectively. Data for I_v and I_p like those shown in Figure 2 were fit with linear regression. As shown in Table 1, the values of σ_v are similar, but not equivalent, for the three different lipid compositions. For PC and PS/PC vesicles, the slopes are equal within experimental uncertainty in the presence and absence of 10 mM Ca^{2+}. For PIP_2/PC vesicles, the slopes are approximately twice as large with, relative to without, 10 mM Ca^{2+}. The value of σ_p was approximately 3-fold higher for b1−94 than for b2−47.

To investigate possible binding of peptides to phospholipid vesicles, small aliquots of peptides were sequentially added to 1.5 mL volumes of phospholipid vesicle suspensions in Tris buffer with 10 mM Ca^{2+} or with 100 mM EDTA. The intensity of scattered light for these samples is $I_{v+p} = I_{vp} + I_p$ where I_{v+p}, I_{vp}, and I_p denote the light scattered by the complete sample, by vesicles containing bound peptides, and

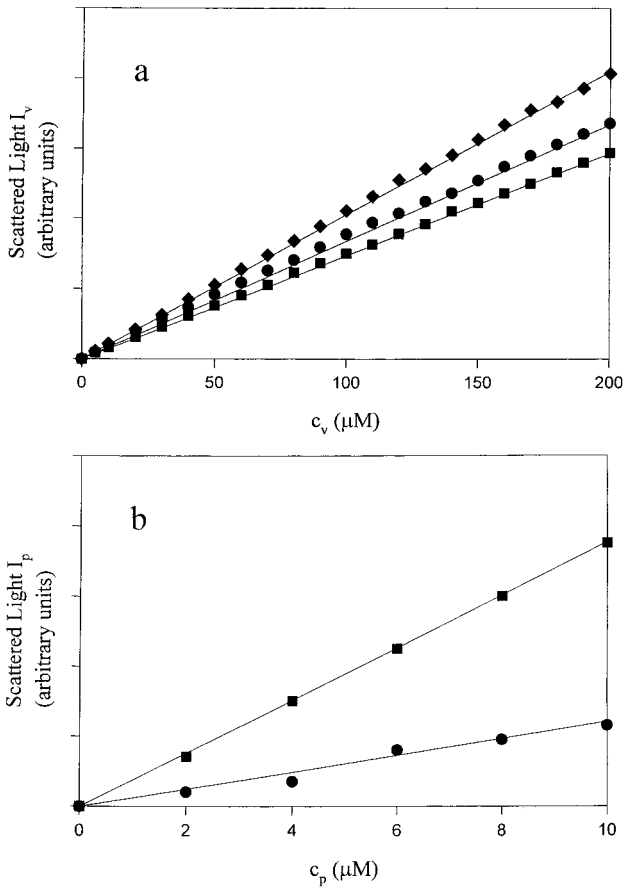

FIGURE 2: Light scattering by vesicles or peptides. The intensity of light scattered by phospholipid vesicles or peptides is linear with the concentration. Representative single trials in Tris buffer without Ca^{2+} are shown for (a) vesicles composed of PC (◆), PS/PC (●), and PIP_2/PC (■); and (b) b1−94 (■) and b2−47 (●) peptides. Data were analyzed by linear regression.

Table 1: Values of σ_v and σ_p Determined by the Concentration Dependence of Scattered Light[a]

sample		$[Ca^{2+}]$ (10 mM)	$\sigma_{v,p}$
vesicles	PC	±	1.00 ± 0.03
	PS/PC	±	0.82 ± 0.02
	PIP_2/PC	+	1.35 ± 0.02
	PIP_2/PC	−	0.71 ± 0.01
peptides	b1−94	±	1.00 ± 0.05
	b2−47	±	0.37 ± 0.07

[a] Data like those shown in Figure 2 were fit to lines to find the best-fit slopes σ_v or σ_p (eq 1). The values of σ_v are equivalent within experimental error for vesicles in the presence of 10 mM Ca^{2+} or 100 mM EDTA, except for PIP_2/PC vesicles where σ_v is larger in the presence of 10 mM Ca^{2+}. Vesicle data are normalized so that $\sigma_v = 1$ for PC; peptide data are normalized so that $\sigma_p = 1$ for b1−94. Values are averages of 2−4 curves for each sample type. Uncertainties are standard deviations of the means.

by free peptides, respectively. The peptide concentrations ranged from 2 to 20 μM, and the phospholipid concentrations were 70 μM. Assuming unilamellar vesicles, and a reasonable minimum of 10 exposed phospholipids per peptide binding site, the maximum concentration of peptide binding sites is 3.5 μM. Thus, the vesicles could significantly deplete the solutions of peptides only for tight binding (calculations not shown), which was not observed (see below). Therefore, to determine I_{vp}, we assumed that the free peptide concentration was equal to the (known) total peptide concentration, I_p was determined from control measurements, and I_{vp} was calculated as $I_{vp} = I_{v+p} - I_p$. Dilution resulting from the addition of aliquots of concentrated peptide solutions was negligible.

The light scattered by vesicles containing bound peptides, relative to the light scattered by vesicles under identical conditions but in the absence of peptides, is *(29−32)*

$$\frac{I_{vp}}{I_v} \approx \left(\frac{M_{vp}}{M_v}\right)^2 \tag{2}$$

where M_{vp} is the molecular weight of vesicles with bound peptides and M_v is the vesicle molecular weight. In the presence of binding, $M_{vp} > M_v$ and $I_{vp}/I_v > 1$; in the absence of binding, $M_{vp} = M_v$ and $I_{vp}/I_v = 1$.

The peptide b1−94 binds PS/PC, PIP_2/PC, and PC vesicles, both in the absence of Ca^{2+} and in the presence of 10 mM Ca^{2+}, as detected by an increase in the light scattered by vesicles in the presence of peptides, after correction for the light scattered by free peptides (Figure 3). Binding was highest for PS/PC vesicles in the presence of Ca^{2+}, and lower for PIP_2/PC vesicles in the absence of Ca^{2+}. For PS/PC vesicles in the absence of Ca^{2+}, PIP_2/PC vesicles in the presence of Ca^{2+}, and PC vesicles in the presence or absence of Ca^{2+}, the excess scattered light was approximately equivalent, nonzero, and less than that for the other two samples. Excess scattered light ($I_{vp} > I_v$) was not detected for the b2−47 peptide for any of the three vesicle compositions, with or without 10 mM Ca^{2+}.

Equation 2 implies that

$$\left(\frac{I_{vp}}{I_v}\right)^{1/2} = 1 + \frac{[P_b]}{[P_b]_\infty} Q \tag{3}$$

where $[P_b]$ is the concentration of bound peptide, $[P_b]_\infty$ is the bound peptide concentration at saturation

$$Q = \frac{M_p}{\beta M_l} \tag{4}$$

M_p and M_l are the peptide and phospholipid molecular weights, respectively, and β is the molar ratio of phospholipid to bound peptide at saturation. The molar concentrations of free peptides, $[P_f]$, were calculated as

$$[P_f] = [P_t] - \left[\left(\frac{I_{vp}}{I_v}\right)^{1/2} - 1\right]\frac{M_l C_v}{M_p} \tag{5}$$

where $[P_t]$ is the total peptide concentration and c_v is the molar concentration of phospholipids. For the tightest binding, b1−94 with PS/PC and 10 mM Ca^{2+}, the free peptide concentrations, $[P_f]$, differed from the total peptide concentrations (2−20 μM) by at most 12%. The values of $[P_f]$ calculated according to eq 5 were used for subsequent data analysis.

It was possible to obtain binding data close to saturation only for b1−94 on PS/PC vesicles in the presence of Ca^{2+} (Figure 3a). For these data, we assume a simple binding mechanism (Appendix):

$$\frac{[P_b]}{[P_b]_\infty} = \frac{[P_f]}{K_d + [P_f]} \tag{6}$$

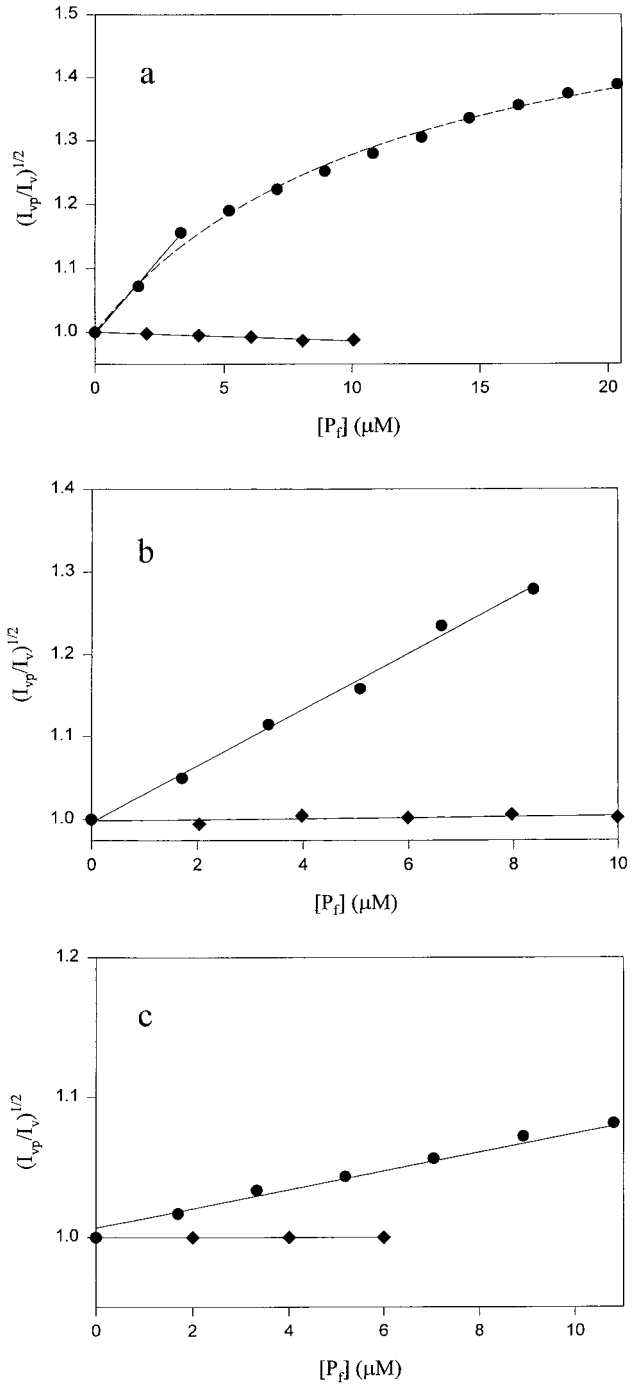

FIGURE 3: Peptide binding to phospholipid vesicles as examined by light scattering. $(I_{vp}/I_v)^{1/2}$ was determined as described in the text. $[P_f]$ is the free peptide concentration (eq 5). Representative single trials are shown for (a) PS/PC with 10 mM Ca^{2+}; (b) PIP_2/PC without Ca^{2+}; and (c) PC with 10 mM Ca^{2+}. Data are shown for b1−94 (●) and b2−47 (◆). Lines show the results of linear regression (eq 7), and the dashed line in (a) shows the best fit to eqs 3 and 6.

where K_d is the apparent equilibrium dissociation constant for the peptide−membrane interaction.[2] The data for b1−94 with PS/PC vesicles and Ca^{2+} were fit to eqs 3 and 6 with K_d and Q as free parameters. This analysis, for five independent sets of data, gave $K_d = 10 \pm 1$ μM and $Q = 0.54 \pm 0.03$. The value of Q, with the known molecular weights of PS, PC, and b1−94, implies that the molar ratio of phospholipid to peptide at saturation is $\beta = 25 \pm 1$. Therefore, for unilamellar vesicles, a single b1−94 binding site consists of approximately 12 phospholipids (9 PC and 3 PS molecules). Assuming an average area per phospholipid of 65 Å^2, the binding site size is ≈780 Å^2 = (28 Å)^2. Considering the known peptide size (94 amino acids), the binding site size could be limited either by the size of the bound peptide or by a specific affinity for 3 PS molecules.

Table 2: Interaction of FcγRIIb1 and FcγRIIb2 Cytoplasmic Peptides with Phospholipid Vesicles[a]

vesicle composition	$[Ca^{2+}]$ (10 mM)	peptide b2−47 slope (mM^{-1})	peptide b1−94 slope(mM^{-1})	peptide b1−94 K_d(μM^{-1})
PS/PC	+	−0.9 ± 1.0	43 ± 7	10 ± 1
PS/PC	−	−0.6 ± 0.1	11 ± 4	39 ± 16
PIP_2/PC	+	−0.1 ± 0.3	8 ± 2	54 ± 17
PIP_2/PC	−	−0.5 ± 0.7	20 ± 4	22 ± 6
PC	+	−0.8 ± 0.8	12 ± 3	36 ± 11
PC	−	−0.1 ± 1.8	14 ± 4	31 ± 11

[a] Data like those shown in Figure 3 were fit to eq 7 to obtain best-fit values of the slopes (shown above) and intercepts (≈1). Slopes are averages of 4−7 curves for each sample type. K_d for PS/PC vesicles in the presence of Ca^{2+} was obtained from data like those shown in Figure 3a; the other K_d values were obtained from the relative values of the slopes (see text). Uncertainties are standard deviations of the means.

For b1−94 with PS/PC vesicles in the absence of Ca^{2+}, and with PIP_2/PC or PC vesicles in the presence or absence of Ca^{2+}, it was not possible to obtain data close enough to saturation for analysis with eqs 3 and 6. Therefore, these data were analyzed with the limiting form of these equations for low peptide concentrations:

$$\left(\frac{I_{vp}}{I_v}\right)^{1/2} \approx 1 + \frac{Q}{K_d}[P_f] \qquad (7)$$

Linear regression was used to obtain best-fit values of the slopes and intercepts. For comparison, the three lowest concentration data points for b1−94 with PS/PC vesicles in the presence of Ca^{2+} were also analyzed in this manner (Figure 3).

For the b1−94 peptide (Table 2), the slopes are highest for PS/PC vesicles in the presence of Ca^{2+}, as expected. The slope for this sample is ≈2-fold higher than the slope for PIP_2/PC vesicles in the absence of Ca^{2+}, and 3-fold to 5-fold higher than the slope for the other four samples. Assuming that β and Q (eq 4) are equivalent to the values measured for PS/PC vesicles in the presence of Ca^{2+}, the decreases in the slopes correspond to equal increases in the equilibrium dissociation constants, giving $K_d \approx 20$ μM and $K_d = 30-50$ μM, respectively. The best-fit values of the intercepts are all approximately 1.

The Ca^{2+} dependence of b1−94 binding to PS/PC vesicles was examined by measuring the excess scattered light for samples with $[P_t] = 10$ μM. $(I_{vp}/I_v)^{1/2}$ increases with added Ca^{2+} as predicted by the results shown in Table 2 (Figure

[2] We cannot rule out the possibility of peptide-induced vesicle aggregation in these measurements, although we have no evidence for its existence. If the observed increase in light scattering is due in part or completely to peptide-mediated vesicle aggregation, this result in itself would demonstrate that the b1−94 peptide interacts with phospholipid surfaces. However, the K_d values estimated from the light scattering data might be distorted by this possible effect. For this reason, the calculated K_d values are reported as apparent equilibrium dissociation constants.

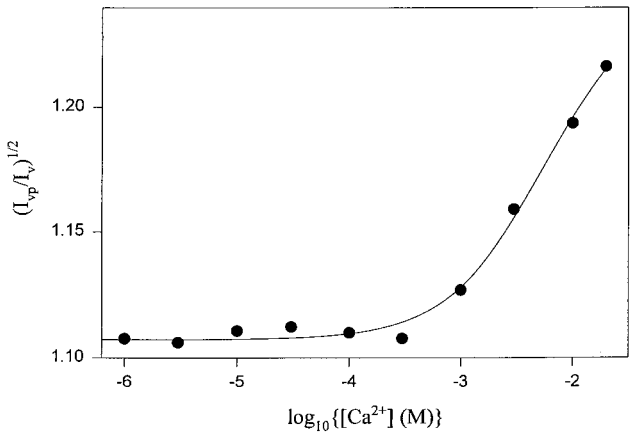

FIGURE 4: Calcium dependence of b1−94 binding to PS/PC phospholipid vesicles. $(I_{vp}/I_v)^{1/2}$ was determined as described in the text. The total peptide concentration was $[P_t] = 10\ \mu M$. A representative single trial is shown with the best fit of the data points to eqs 3 and 8.

4). Control measurements demonstrate that the light scattered by solutions containing only vesicles, I_v, does not change with added Ca^{2+} up to 20 mM. Data like those shown in Figure 4 were analyzed by assuming that Ca^{2+} binds either to the peptides or to the membranes, decreasing the peptide−membrane equilibrium dissociation constant. For these models (Appendix), $(I_{vp}/I_v)^{1/2}$ is given by eq 3 with

$$\frac{[P_b]}{[P_b]_\infty} = \frac{[P_f]}{K_d([Ca^{2+}]) + [P_f]}$$

$$K_d([Ca^{2+}]) = \left[\frac{K_c}{K_c + [Ca^{2+}]}\frac{1}{K_d(0)} + \frac{[Ca^{2+}]}{K_c + [Ca^{2+}]}\frac{1}{K_d(\infty)}\right]^{-1} \quad (8)$$

where $K_d(0)$ and $K_d(\infty)$ are the apparent peptide−membrane equilibrium dissociation constants in the absence of Ca^{2+} and the presence of high Ca^{2+} concentrations, respectively; and K_c is the apparent equilibrium dissociation constant for Ca^{2+} and peptides, or for Ca^{2+} and phospholipids. The data were fit to eqs 3 and 8 (Figure 4). $[P_f]$ was fixed at the value given by eq 5, Q was set at 0.54, and the free parameters were K_c, $K_d(0)$, and $K_d(\infty)$. This analysis, averaged over four data sets, gave $K_d(\infty) = 14 \pm 6\ \mu M$, $K_d(0) = 55 \pm 20\ \mu M$, and $K_c = 10 \pm 3$ mM. These values of K_d are consistent with the ones in Table 2.

The Ca^{2+} dependence of b1−94 binding to PIP_2/PC vesicles was also examined by measuring the excess scattered light for samples with $[P_t] = 10\ \mu M$ (data not shown). Unlike the results for PS/PC vesicles, the intensity of light scattered by vesicles in the absence of peptide, I_v, increased significantly with added Ca^{2+}. This increase was most pronounced for Ca^{2+} concentrations greater than 1 mM. I_{vp} was greater than I_v at low Ca^{2+} concentrations (<0.1 mM), but less than I_v at high Ca^{2+} concentrations (>1 mM). These results suggest that Ca^{2+} induces significant aggregation or fusion of PIP_2/PC vesicles and that b1−94 alters this process.

For b2−47, no increase in the light scattered by vesicles in the presence of peptides, after correction for the light scattered by free peptides, was observed for any of the three phospholipid compositions, in the presence or absence of Ca^{2+} (Figure 3). The slopes, as determined by fitting to eq 7, are not statistically different from zero, and the intercepts are approximately 1 (Table 2). The lack of detectable, increased scattered light is not a consequence of the smaller molecular weight of b2−47 relative to b1−94, as the difference in molecular weight would reduce the slope only by a factor of 2 (eq 4).

The most prominent difference between the b1−94 and b2−47 peptides is the 48 amino acid replacement in b1−94 of a single amino acid residue in b2−47 (Figure 1). However, the b1−94 peptide also contains a methionine and six histidines not present in the b2−47 peptide. It is unlikely that the histidine tag alters the b1−94 peptide conformation in such a manner that an artifactual phospholipid binding site is generated. Histidine tags rarely interfere with the structure or function of proteins to which they are conjugated *(33−36)*. To rule out the possibility that the six histidine residues, by themselves, are responsible for the membrane binding properties of b1−94, light scattering measurements were carried out for an unrelated ≈10 kDa protein that also contains a six-residue histidine tag, the protease inhibitor eglin c. The control measurements were carried out for PS/PC and PC vesicles in the presence and absence of 10 mM Ca^{2+}. No increase in the light scattered by vesicles in the presence of this protein, after correction for the light scattered by free protein, was observed. This result, that the histidine tag alone does not induce membrane binding, is consistent with previous work demonstrating that proteins containing histidine tags bind to phospholipid membranes only when the membranes contain specific phospholipids with nickel-chelating headgroups *(37−39)*.

DISCUSSION

Recent work has begun to dissect the manner in which the two forms of mFcγRII, which differ only in the cytoplasmic region, participate in signal transduction (*1−25)*. Both proteins mediate the phagocytosis of opsonized particulate matter. However, only mFcγRIIb2 mediates coated pit localization and subsequent internalization of soluble immune complexes. The insertion in mFcγRIIb1 is thought to prevent coated pit localization by a direct interaction with the cytoskeleton. In B cells, mFcγRIIb1 prevents cellular activation in response to antigen. Similar inhibitory roles for mFcγRIIb1 have also been identified in other cell types such as T cells and mast cells.

The data in Figure 3 and Table 2 demonstrate that the isolated cytoplasmic region of mFcγRIIb1 binds phospholipid membrane surfaces, whereas the isolated cytoplasmic region of mFcγRIIb2 does not. This result suggests that the mechanism by which the cytoplasmic region of mFcγRIIb1 transduces signals may rely in part on the influence of the nearby membrane surface. The most prominent difference between the b1−94 and b2−47 peptides is the 48 amino acid replacement in b1−94 of a single amino acid residue in b2−47 (Figure 1), suggesting that the insert mediates membrane binding. It is unlikely that the electrostatic properties of the two peptides account for the difference in membrane binding (specifically, to negatively charged membrane surfaces). Both peptides are negatively charged, and the b2−47 peptide is less negatively charged (−7) than the b1−94 peptide (−11).

Considerable attention has been focused on the tyrosine residues in the mFcγRIIb1 and mFcγRIIb2 cytoplasmic regions because these residues may play a role in regulating signal transduction. The cytoplasmic region of mFcγRIIb1 contains four tyrosine residues at positions 28, 54, 73, and 90 from the membrane, whereas the cytoplasmic region of mFcγRIIb2 contains only two tyrosines at positions 26 and 43. One of these tyrosine residues (position 73 in mFcγRIIb1 and position 26 in mFcγRIIb2) is contained in the ITIM (Figure 1). This motif is implicated in the endocytosis of soluble immune complexes as mediated by mFcγRIIb2 *(8−12)* and is also responsible for the inhibition by FcγRIIb1 of cellular activation *(12−25)*. Because the ITIM motif is found in both mFcγRIIb1 and mFcγRIIb2, this motif is unlikely to be directly responsible for membrane binding.

Although the apparent membrane equilibrium dissociation constant for b1−94 is rather high (10−55 μM), this peptide in vivo is necessarily proximal to the cytoplasmic membrane face because of its covalent attachment to the transmembrane region of mFcγRIIb1. Therefore, the cytoplasmic region of mFcγRIIb1 almost certainly interacts directly with the phospholipid surface. Previous work has demonstrated that the b1−94 peptide, a rather large ≈10 kDa peptide, is largely unstructured in aqueous solutions but that nonaqueous solvents such as trifluoroethanol and methanol induce significant structure *(26)*. Therefore, the result that b1−94 binds to phospholipid membranes suggests that this nearby surface may be crucial to the in vivo structure of the cytoplasmic region of mFcγRIIb1.

A variety of cytoplasmic proteins reversibly associate with the cytoplasmic face of plasma membranes during cellular signaling. Proteins such as the myristoylated alanine-rich C kinase substrate associate with the plasma membrane through a combination of a hydrophobic interaction between the fatty acid and membrane, and an electrostatic interaction between positively charged amino acids and negatively charged phospholipids; upon phosphorylation, the electrostatic interaction is reduced and the proteins dissociate from the membrane *(40)*. For other myristoylated proteins, like recoverin, Ca^{2+} binding exposes the fatty acid and induces membrane binding *(41)*. A variety of nonmyristoylated intracellular proteins contain the ≈130-residue C2 domain, which is thought to be responsible for Ca^{2+}-induced association with the cytoplasmic face of the plasma membrane *(42)*.

The apparent equilibrium dissociation constant for the binding of the soluble b1−94 peptide to phospholipid vesicles depends both on the phospholipid composition and on the Ca^{2+} concentration (Table 2, Figures 3 and 4). In the absence of Ca^{2+}, b1−94 binds more tightly to PIP_2/PC (25/75, mol/mol) vesicles ($K_d \approx 22$ μM) than to PS/PC (25/75, mol/mol) or PC vesicles ($K_d = 35-40$ μM); in the presence of 10 mM Ca^{2+}, b1−94 binds more tightly to PS/PC vesicles ($K_d \approx 10$ μM) than to PIP_2/PC or PC vesicles ($K_d = 35-55$ μM); 10 mM Ca^{2+} decreases the apparent, equilibrium dissociation constant of b1−94 with PS/PC (25/75, mol/mol) vesicles, increases the apparent equilibrium dissociation constant of b1−94 with PIP_2/PC (25/75, mol/mol) vesicles, and does not change the apparent equilibrium dissociation constant of b1−94 with pure PC vesicles within experimental uncertainty.

The result that the association of the soluble b1−94 peptide with vesicles depends on the phospholipid composition and the Ca^{2+} concentration suggests that the cytoplasmic region of mFcγRIIb1 (and perhaps other transmembrane proteins) might reversibly associate with membrane surfaces during cellular response to external signals in a manner similar to soluble intracellular proteins such as those containing C2 domains. The density of PS (25 mol %) in the phospholipid vesicles is within the known physiological range for some cell types *(31)*. Although the density of PIP_2 (25 mol %) in the phospholipid vesicles is much higher than its density in natural membranes, PIP_2 may not be homogeneously distributed in natural membranes. Instead, it might be present in domains where the local density is high *(43, 44)*. However, the concentrations of Ca^{2+} which alter the binding of soluble b1−94 to phospholipid vesicles (millimolar) are much larger than typical intracellular Ca^{2+} concentrations during cellular signaling (micromolar) *(13, 24, 45−48)*. Because the Ca^{2+} concentrations at which membrane binding is modulated are not physiological, the PIP_2 densities may not be physiological, and the effects of phospholipid composition and Ca^{2+} concentration are modest, it seems unlikely that these effects will be significant in intact cells. More likely is the case that the mFcγRIIb1 cytoplasmic region is present in intact cells in a membrane-bound state, and that the strength of this binding is not significantly affected by PS, PIP_2, or Ca^{2+}.

We have demonstrated that the soluble peptide corresponding to the cytoplasmic region of mFcγRIIb1 binds to phospholipid membrane surfaces, whereas the soluble peptide corresponding to the cytoplasmic region of mFcγRIIb2 does not. Because these peptides are covalently attached to the plasma membrane in vivo, the results strongly suggest that the cytoplasmic region of mFcγRIIb1 is in the membrane-bound state in intact cells. Because this peptide has very little structure in aqueous solution *(26)*, it is possible that the membrane surface confers structure on this peptide. The association of the b1−94 peptide with phospholipid vesicles is weakly dependent on the phospholipid composition and Ca^{2+} concentration, raising the possibility that membrane binding by the mFcγRIIb1 cytoplasmic region might be modulated by these factors in vivo. However, the required concentrations of PIP_2 and Ca^{2+} are much higher than physiological concentrations, and the effects of PS, PIP_2, and Ca^{2+} on the apparent equilibrium dissociation constants are small. Thus, the degree to which the mFcγRIIb1 cytoplasmic region binds to the plasma membrane is not likely to be significantly modified by these factors.

ACKNOWLEDGMENT

We thank Jinkeun Lee and Barry R. Lentz for assistance with the phosphate assay, and Jennifer L. Waldner for providing the his-tag control protein.

APPENDIX: MODELS FOR PEPTIDE−MEMBRANE BINDING

In the simplest model where peptides reversibly associate with sites on vesicle surfaces, the equilibrium is described by

$$[P_f][L] = K_d[P_b]$$
$$[P_b]_\infty = [L] + [P_b] \quad \text{(A1)}$$

where $[P_f]$ and $[P_b]$ are the concentrations of peptides free in solution and bound to vesicle surfaces, [L] is the concentration of free membrane binding sites, and $[P_b]_\infty$ is

the concentration of bound peptides at saturation. Equations A1 imply eq 6.

If Ca^{2+} binds to peptides, enhancing the membrane interaction, the equilibrium is described by

$$[A][L] = K_d(0)[B]$$

$$[A^*][L] = K_d(\infty)[B^*]$$

$$[A][Ca^{2+}] = K_c[A^*]$$

$$[P_f] = [A] + [A^*]$$

$$[P_b] = [B] + [B^*]$$

$$[P_b]_\infty = [L] + [B] + [B^*] \quad \text{(A2)}$$

where [A] and [A*] are the concentrations of peptides free in solution, uncomplexed and complexed with Ca^{2+}, respectively; and [B] and [B*] are the concentrations of bound peptides, uncomplexed and complexed with Ca^{2+}, respectively. $K_d(0)$ is the equilibrium dissociation constant for uncomplexed peptides and free membrane binding sites, $K_d(\infty)$ is the equilibrium dissociation constant for complexed peptides and membrane binding sites, and K_c is the equilibrium dissociation constant for peptides and Ca^{2+}. Equations A2 imply eqs 8.

If Ca^{2+} binds to the phospholipid vesicles, enhancing their interaction with peptides, the equilibrium is described by

$$[P_f][L] = K_d(0)[B]$$

$$[P_f][L^*] = K_d(\infty)[B^*]$$

$$[L][Ca^{2+}] = K_cL^*$$

$$[P_b] = [B] + [B^*]$$

$$[P_b]_\infty = [L] + [L^*] + [B] + [B^*] \quad \text{(A3)}$$

where [L] and [L*] are the concentrations of vesicle binding sites, uncomplexed and complexed with Ca^{2+}, respectively; and K_c is the equilibrium dissociation constant for phospholipids and Ca^{2+}. Equations A3 also imply eqs 8.

REFERENCES

1. Fridman, W. H., Bonnerot, C., Daëron, M., Amigorena, S., Teillaud, J.-L., and Sautes, C. (1992) *Immunol. Rev. 125*, 49−76.
2. Hulett, M. D., and Hogarth, P. M. (1994) *Adv. Immunol. 57*, 1−127.
3. Indik, Z. K., Park, J.-G., Hunter, S., and Schreiber, A. D. (1995) *Blood 86*, 4389−4399.
4. Ravetch, J. V. (1997) *Curr. Opin. Immunol. 9*, 121−125.
5. Isakov, N. (1997) *J. Leukocyte Biol. 61*, 6−16.
6. Isakov, N. (1997) *Immunol. Res. 16*, 85−100.
7. Daëron, M. (1997) *Annu. Rev. Immunol. 15*, 203−234.
8. Miettinen, H. M., Rose, J. K., and Mellman, I. (1989) *Cell 58*, 317−327.
9. Miettinen, H. M., Matter, K., Hunziker, W., Rose, J. K., and Mellman, I. (1992) *J. Cell Biol. 116*, 875−888.
10. Hunziker, W., and Fumey, C. (1994) *EMBO J. 13*, 2963−2967.
11. Daëron, M., Malbec, O., Latour, S., Bonnerot, C., Segal, D. M., and Fridman, W. H. (1993) *Int. Immunol. 5*, 1393−1401.
12. Amigorena, S., Bonnerot, C., Drake, J. R., Choquet, D., Hunziker, W., Guillet, J. G., Webster, P., Sautes, C., Mellman, I., and Fridman, W. H. (1992) *Science 256*, 1808−1812.
13. Choquet, D., Partiseti, M., Amigorena, S., Bonnerot, C., Fridman, W. H., and Korn, H. (1993) *J. Cell Biol. 121*, 355−363.
14. Weiss, A., and Littman, D. R. (1994) *Cell 76*, 263−274.
15. Muta, T., Kurosaki, T., Misulovin, Z., Sanchez, M., Nussenzweig, M. C., and Ravetch, J. V. (1994) *Nature 368*, 70−73.
16. D′Ambrosio, D., Hippen, K. L., Minskoff, S. A., Mellman, I., Pani, G., Siminovitch, K. A., and Cambier, J. C. (1995) *Science 268*, 293−297.
17. Daëron, M., Latour, S., Malbec, O., Espinosa, E., Pina, P., Pasmans, S., and Fridman, W. H. (1995) *Immunity 3*, 635−646.
18. Daëron, M., Malbec, O., Latour, S., Espinosa, E., Pina, P., and Fridman, W. H. (1995) *Immunol. Lett. 44*, 119−123.
19. Van den Herik-Oudijk, I. E., Capel, P. J. A., Van der Bruggen, T., and Van de Winkel, J. G. (1995) *Blood 85*, 2202−2211.
20. Scharenberg, A. M., and Kinet, J.-P. (1996) *Cell 87*, 961−964.
21. Cassard, S., Choquet, D., Fridman, W. H., and Bonnerot, C. (1996) *J. Biol. Chem. 271*, 23786−23791.
22. Nadler, M. J. S., Chen, B., Anderson, J. S., Wortis, H. H., and Neel, B. G. (1997) *J. Biol. Chem. 272*, 20038−20043.
23. Gupta, N., Scharenberg, A. M., Burshtyn, D. N., Wagtmann, N., Lioubin, M. N., Rohrschneider, L. R., Kinet, J. P., and Long, E. O. (1997) *J. Exp. Med. 186*, 473−478.
24. Hippen, K. L., Buhl, A. M., D′Ambrosio, D., Nakamura, K., Persin, C., and Cambier, J. C. (1997) *Immunity 7*, 49−58.
25. Sarmay, G., Koncz, G., Pecht, I., and Gergely, J. (1997) *Immunol. Lett. 57*, 159−164.
26. Chen, L., Thompson, N. L., and Pielak, G. J. (1997) *Protein Sci. 6*, 1038−1046.
27. Waldner, J. C., Lahr, S. J., Edgell, M. H., and Pielak, G. J. (1998) *Anal. Biochem. 263*, 116−118.
28. Chen, P. S., Toribara, T. Y., and Warner, H. (1956) *Anal. Chem. 28*, 1756−1758.
29. Nelsestuen, G. L., and Lim, T. K. (1977) *Biochemistry 16*, 4164−4171.
30. Cutsforth, G. A., Whitaker, R. N., Hermans, J., and Lentz, B. R. (1989) *Biochemistry* 28, 7453−7461.
31. Pearce, K. H., Hiskey, R. G., and Thompson, N. L. (1992) *Biochemistry 31*, 5983−5995.
32. Han, X., Li, G., Li, G., and Lin, K. (1997) *Biochemistry 36*, 10364−10371.
33. Qian, X., Gozani, S. N., Yoon, H., Jeon, C. J., Agarwal, K., and Weiss, M. A. (1993) *Biochemistry 32*, 9944−9959.
34. Dobeli, H., Trecziak, A., Gillessen, D., Matile, H., Srivastava, I. K., Perrin, L. H., Jakob, P. E., and Certa, U. (1990) *Mol. Biochem. Parasitol. 41*, 259−268.
35. Janknecht, R., de Martynoff, G., Lou, J., Hipskind, R. A., Nordheim, A., and Stunnenberg, H. G. (1991) *Proc. Natl. Acad. Sci. U.S.A. 88*, 8972−8976.
36. Takacs, B. J., and Giraud, M. F. (1991) *J. Immunol. Methods 143*, 231−240.
37. Barklis, E., McDermott, J., Wilkens, S., Schabtach, E., Schmid, M. F., Fuller, S., Karanjia, S., Love, Z., Jones, R., Rui, Y., Zhao, X., and Thompson, D. (1997) *EMBO J. 16*, 1199−1213.
38. Dietrich, C., Schmitt, L., and Tampe, R. (1995) *Proc. Natl. Acad. Sci. U.S.A. 92*, 9014−9018.
39. Ng, K., Pack, D., Sasaki, D., and Arnold, F. (1995) *Langmuir 11*, 4048−4055.
40. McLaughlin, S., and Aderem, A. (1995) *Trends Biochem. Sci. 20*, 272−276.
41. Ames, J. B., Ishima, R., Tanaka, T., Gordon, J. I., Stryer, L., and Ikura, M. (1997) *Nature 389*, 198−202.
42. Nalefski, E. A., and Falke, J. J. (1996) *Protein Sci. 5*, 2375−2390.
43. Pike, L. J., and Casey, L. (1996) *J. Biol. Chem. 271*, 26453−26456.

44. Denisov, G., Wanaski, S., Luan, P., Glaser, M., and McLaughlin, S. (1998) *Biophys.* J. 74, 731−744.
45. Nagahata, H., Sawada, C., Higuchi, H., Teraoka, H., and Yamaguchi, M. (1997) *Microbiol. Immunol. 41*, 747−750.
46. Strohmeier, G. R., Brunkhorst, B. A., Seetoo, K. F., Bernardo, J., Weil, G. J., and Simons, E. R. (1995) *J. Leukocyte Biol. 58*, 403−414.
47. Lang, M. L., Glennie, M. J., and Kerr, M. A. (1997) *Biochem. Soc. Trans. 25*, 333S.
48. Qi, R., Ozaki, Y., Kuroda, K., Asazuma, N., Yatomi, Y., Satoh, K., Nomura, S., and Kume, S. (1996) *J. Immunol. 157*, 5638−5645.

BI980683J